Spin-charge coupling in quantum wires at zero magnetic field

Rodrigo G. Pereira[1,2] and Eran Sela[3]
[1]*Kavli Institute for Theoretical Physics, University of California, Santa Barbara, California 93106, USA*
[2]*Instituto de Fíisica de São Carlos, Universidade de São Paulo, CP 369, São Carlos 13566-970, SP, Brazil*
[3]*Institute for Theoretical Physics, University of Cologne, 50937 Cologne, Germany*
(Received 7 November 2009; revised manuscript received 14 June 2010; published 27 September 2010)

We discuss an approximation for the dynamic charge response of nonlinear spin-1/2 Luttinger liquids in the limit of small momentum. Besides accounting for the broadening of the charge peak due to two-holon excitations, the nonlinearity of the dispersion gives rise to a two-spinon peak, which at zero temperature has an asymmetric line shape. At finite temperature the spin peak is broadened by diffusion. As an application, we discuss the density and temperature dependence of the Coulomb drag resistivity due to long-wavelength scattering between quantum wires.

DOI: 10.1103/PhysRevB.82.115324 PACS number(s): 73.63.Nm, 71.10.Pm

I. INTRODUCTION

There is theoretical consensus,[1] supported by accumulating experimental evidence,[2,3] that in one dimension electrons decay into fractional excitations carrying either spin or charge, called spinon and holon. At low energies, interacting one-dimensional systems are described by the Luttinger model,[1] which predicts that the collective spin and charge modes are decoupled and propagate with different velocities. Away from the low-energy limit, spin-charge separation holds in the sense that spinon and holon branches can still be identified in some momentum-resolved experiments such as angle-resolved photoemission[4] but charge and spin degrees of freedom are inevitably coupled by dispersion nonlinearity. A direct consequence is that at finite energies spin excitations can contribute to charge responses.[5,6]

Recently the effects of nonlinear dispersion in dynamical properties of Luttinger liquids have been emphasized.[7] In particular, the interplay of band curvature and interactions is essential for the interpretation of Coulomb drag experiments in parallel quantum wires.[8,9] As discussed by Pustilnik *et al.*,[10] the Luttinger model cannot account for the leading contribution to the drag resistivity when there is a density mismatch between the wires, in which case interwire backscattering processes are exponentially suppressed at low temperatures. The other type of low-energy process, long-wavelength scattering, is ineffective within the Luttinger model because the dynamic charge-structure factor (DCSF) $S(q,\omega)$ for small wave vector q is given by a delta function peak at the energy of a free boson. In this approximation, the DCSFs of two wires with different densities have no overlap and the drag resistivity vanishes. For *spinless* fermions,[10] it is known that nonlinear dispersion is responsible for broadening the DCSF into a rectangular line shape with width proportional to q^2.[11,12] This effect restores a smooth density dependence of the drag resistivity.

In this work we study the DCSF of spin-1/2 fermions in the limit of small q and at zero magnetic field. Our motivation comes from the search for Luttinger liquid behavior in experiments with vertically coupled quantum wires, in which drag is enhanced by a smaller interwire separation and the densities in each wire can be tuned independently.[13] We are interested in the possibility that spinons give a contribution to the drag resistivity via spin-charge coupling at finite energies. This effect cannot be described by the Luttinger model since it depends on violating particle-hole symmetry. In order to calculate the DCSF, we follow the approach of treating band curvature as a perturbation to the Luttinger model, and resort to refermionization of the collective modes in the cases where perturbation theory is singular. While the drag response depends mostly on the spectral weight and width of the peaks as a function of wave vector and temperature, we also discuss other features of the DCSF that are of general interest for the dynamics of spin-1/2 fermions. These features could be directly probed by momentum-resolved techniques, such as Bragg spectroscopy in cold Fermi gases.[14] We show that at zero temperature the charge peak has a q^2-scaling width, such as in the spinless case, but there is also a peak due to spin excitations which resembles the dynamic spin structure factor (DSSF) of Heisenberg spin chains. At zero temperature, the DCSF diverges at the lower edge of the spin peak as a power law with exponent $\mu_{s-}=-1/2+\mathcal{O}(q^2)$. At finite temperature, the spin peak is broadened by diffusion.

The paper is organized as follows. In Sec. II we present the linear-response formula for the drag resistivity and discuss its relation to the problem of the DCSF of spin-1/2 fermions with nonlinear dispersion. In Sec. III, we derive the effective bosonic Hamiltonian including irrelevant operators associated with band curvature, some of which couple charge and spin degrees of freedom. In Sec. IV, we describe the line shape of the DCSF in the limit of small q at zero temperature. Finite temperature effects are also discussed. In Sec. V, the approximation for the DCSF is applied to calculate the density and temperature dependence of the drag resistivity. Finally, we summarize the results in Sec. VI.

II. COULOMB DRAG AND DYNAMIC CHARGE RESPONSE

The drag resistivity between two capacitively coupled wires of length L is defined as the ratio $r=-(e^2/2\pi\hbar)V_2/I_1L$, where V_2 is the voltage induced across wire 2 (called the drag wire) when a current I_1 is driven

through wire 1 (called the drive wire). For the typical setup, see Refs. 8 and 9. Let us assume clean wires (L smaller than the mean-free path due to impurities) and temperature regime $k_BT \gg \hbar v_{Fi}/L$, where v_{Fi}, $i=1,2$, is the Fermi velocity for electrons in each wire. The latter condition rules out finite size effects which are known to produce oscillations in the drag response as a function of drive voltage.[15] Hereafter we set $\hbar=k_B=1$. In the linear-response regime, the drag resistivity at temperature T is given by[10]

$$r = \frac{U^2}{4\pi^3 \nu_1 \nu_2 T} \int_0^\infty dq \int_0^\infty d\omega \frac{q^2 A_1(q,\omega) A_2(q,\omega)}{\sinh^2(\omega/2T)}, \quad (1)$$

where U is the interwire Coulomb interaction, ν_i is the charge density and $A_i(q,\omega)$ is minus the imaginary part of the retarded density-density correlation function in wire $i=1,2$. Equation (1) expresses the drag resistivity as a functional of the dynamic density-density correlation function of two decoupled wires. Due to Boltzmann factors, the nonzero response comes from the overlap of A_1 and A_2 integrated up to frequencies of order T. At low temperatures compared to the Fermi energies ϵ_{Fi} of the wires, and neglecting interwire backscattering, the main contribution to the integral in Eq. (1) is due to small-q (or forward) scattering.[10]

Our goal is to derive an approximation for $A(q,\omega)$ in a single wire in the limit $q \ll k_{Fi}$ and $\omega \ll \epsilon_{Fi}$. From this point until Sec. IV, we will be concerned with the dynamic response of a single wire and will omit the wire index $i=1,2$. The wire index will be restored in Sec. V when we return to Eq. (1) to compute the drag resistivity.

In order to describe the intrawire interactions, we consider a Galilean-invariant model with electron mass m and short-range density-density interaction potential $V(x)$

$$H = -\frac{1}{2m} \int_0^L dx \Psi^\dagger \partial_x^2 \Psi + \frac{1}{2} \int_0^L dx \int_0^L dy V(x-y) n(x) n(y). \quad (2)$$

Here $\Psi=(\psi_\uparrow,\psi_\downarrow)$ is a two-component fermionic field and $n(x)=\Psi^\dagger(x)\Psi(x)$ is the local charge density. At zero magnetic field, the number of electrons with spin $\sigma=\uparrow,\downarrow$ is $N_\uparrow=N_\downarrow=N/2$. The average density is $\nu=N/L$ and the Fermi wave vector is $k_F=\pi\nu/2$. We assume the interaction potential to have a finite range R, due to screening by nearby gates. For simplicity, we will discuss the properties of $A(q,\omega)$ in the thermodynamic limit.

The spectral function $A(q,\omega)$ in Eq. (1) satisfies the fluctuation-dissipation theorem

$$2A(q,\omega) = (1 - e^{-\omega/T}) S(q,\omega), \quad (3)$$

where $S(q,\omega)$ is the DCSF given by

$$S(q,\omega) = \int_0^L dx e^{-iqx} \int_{-\infty}^{+\infty} dt e^{i\omega t} \langle n(x,t) n(0,0) \rangle. \quad (4)$$

Since $S(-q,\omega)=S(q,\omega)$, hereafter we take $q>0$. Since we are interested in the regime $T \ll \epsilon_F$, we shall start by discussing the DCSF at $T=0$. The exact result for the noninteracting case, $V=0$, is

$$S_0(q,\omega) = (2m/q)\,\theta(q^2/2m - |\omega - v_F q|), \quad (5)$$

where $v_F=k_F/m$ is the Fermi velocity. For $V=0$, the spectral weight vanishes outside the particle-hole continuum defined by the upper and lower thresholds $\omega_\pm(q)=v_F q \pm q^2/2m$. As a function of energy ω, the line shape of the DCSF in this case consists of one rectangular peak whose width is given by the band curvature scale $\delta\omega(q)=q^2/m$.

It is important to note that for spin-1/2 fermions the DCSF at small q cannot be obtained by perturbation theory in the interaction. In fact, the first-order correction to $S(q,\omega)$ has logarithmic divergences at $\omega \approx \omega_\pm(q)$

$$\frac{\delta S(q,\omega)}{S_0(q,v_F q)} \approx \frac{m(2\tilde{V}_q - \tilde{V}_0)}{\pi q} \ln \left| \frac{\omega - \omega_-}{\omega_+ - \omega} \right|, \quad (6)$$

where $\tilde{V}_k$ is the Fourier transform of $V(x)$. These divergences signal edge singularities and are reminiscent of the result for spinless fermions[16] but there is an important difference. For spinless fermions, the prefactor of the logarithmic divergence is $-m(\tilde{V}_0-\tilde{V}_q)/\pi q$; for short-range interactions, $\tilde{V}_0-\tilde{V}_q \sim q^2$, it vanishes as $q \to 0$. In contrast, the prefactor in the spinful case, $m(2\tilde{V}_q-\tilde{V}_0)/\pi q \approx m\tilde{V}_0/\pi q$, diverges as $q \to 0$. The difference stems from the amplitude for s-wave scattering between electrons with opposite spin. This indicates that the limits $q \to 0$ and $\tilde{V}_0 \to 0$ in $S(q,\omega)$ do not commute. In the limit $q \ll m\tilde{V}_0$, it is important to treat interactions exactly and account for the effects of spin-charge separation, as we will discuss in the following sections.

III. EFFECTIVE MODEL FOR SPIN-CHARGE COUPLING

In the regime $q \ll m\tilde{V}_0$, we can treat interactions exactly and regard band curvature as a perturbation, with q/k_F playing the role of a small parameter.[12,17,18] In the linear dispersion approximation, bosonization[1] of Hamiltonian (2) is standard and leads to the Luttinger model with Hamiltonian density

$$\mathcal{H}_\ell = 2\pi v_c (J_R^2 + J_L^2) + \frac{2\pi v_s}{3} (\mathbf{J}_R^2 + \mathbf{J}_L^2) - 2\pi v_s g \mathbf{J}_R \cdot \mathbf{J}_L. \quad (7)$$

Here $J_{R/L}$ ($\mathbf{J}_{R/L}$) are chiral U(1) charge [SU(2) spin] currents, v_c (v_s) is the charge (spin) velocity, and g is the bare coupling constant of the marginally irrelevant backscattering operator. The long-wavelength part of the charge density fluctuation is

$$n = 2\sqrt{K_c}(J_R + J_L), \quad (8)$$

where K_c is the Luttinger parameter for the charge sector. Galilean invariance implies $K_c=v_F/v_c$. At weak coupling, $\tilde{V}_0 \ll v_F$, we have $v_c \approx v_F + \tilde{V}_0/\pi$, $v_s \approx v_F$, and $g \approx \tilde{V}_{2k_F}/\pi v_F$.[1] In semiconductor quantum wires, typical values of $K_c \approx 0.7$ have been reported.[3]

The charge and spin currents can be expressed in terms of chiral bosonic fields as

$$J_{R/L} = \mp \partial_x \varphi^c_{R/L}/\sqrt{4\pi}, \quad (9)$$

$$J^z_{R/L} = \mp \partial_x \varphi^s_{R/L}/\sqrt{4\pi}, \tag{10}$$

which obey the commutation relations $[\varphi^c_{R/L}(x), \partial_{x'}\varphi^c_{R/L}(x')] = [\varphi^s_{R/L}(x), \partial_{x'}\varphi^s_{R/L}(x')] = \mp i\delta(x-x')$. The transverse part of the spin currents can be written as

$$J^+_{R/L} = J^x_{R/L} + iJ^y_{R/L} = \frac{1}{2\pi} e^{+i\sqrt{4\pi}\varphi^s_{R/L}}, \tag{11}$$

$$J^-_{R/L} = J^x_{R/L} - iJ^y_{R/L} = \frac{1}{2\pi} e^{-i\sqrt{4\pi}\varphi^s_{R/L}}, \tag{12}$$

where the short-distance cutoff is set to 1.

The leading (dimension-three) perturbations to the model in Eq. (7), generated by the quadratic term in the electron dispersion as well as irrelevant interactions, are

$$\begin{aligned}\delta\mathcal{H} = (4\pi^2/3)[&\eta_-(J^3_R + J^3_L) - \eta_+(J^2_R J_L + J^2_L J_R) \\ &+ \kappa_-(J_R \mathbf{J}^2_R + J_L \mathbf{J}^2_L) + \kappa_+(J_R \mathbf{J}^2_L + J_L \mathbf{J}^2_R) \\ &+ \kappa_3(J_L + J_R)\mathbf{J}_L \cdot \mathbf{J}_R].\end{aligned} \tag{13}$$

The last three terms in Eq. (13) couple spin and charge. Importantly, only even powers of the spin currents are allowed in $\delta\mathcal{H}$ due to SU(2) symmetry. Direct bosonization of Hamiltonian (2) produces all terms in Eq. (13), except for the κ_3 term. This does not mean that κ_3 vanishes (such term is allowed by symmetry) but rather that it must be generated at second order in the electron-electron interaction.

In fact, we can derive phenomenological relations for all coupling constants. The exact parameters $\eta_\pm$ can be related to the change of v_c and K_c under a shift of chemical potential μ. The calculation is analogous to the spinless case in Ref. 12; simplifying for the case of Galilean invariance where $K_c = v_F/v_c$ and using the result for the compressibility $\partial\nu/\partial\mu = 2K_c/\pi v_c$, we find

$$\eta_- = \frac{1}{2\sqrt{K_c}}\left(\frac{1}{m} + v_c\frac{\partial v_c}{\partial\mu}\right), \tag{14}$$

$$\eta_+ = \frac{3}{2\sqrt{K_c}}\left(\frac{1}{m} - v_c\frac{\partial v_c}{\partial\mu}\right). \tag{15}$$

Likewise, an infinitesimal chemical potential shift $\delta\mu$ modifies the spin velocity v_s by giving a finite expectation value to the charge currents $\langle J_L\rangle = \langle J_R\rangle = \delta\mu\sqrt{K_c}/(2\pi v_c)$ in the $\kappa_\pm$ terms in Eq. (13)

$$\frac{4\pi^2}{3}(\kappa_- + \kappa_+)\langle J_R\rangle(\mathbf{J}^2_R + \mathbf{J}^2_L) \equiv \frac{2\pi}{3}\delta v_s(\mathbf{J}^2_R + \mathbf{J}^2_L). \tag{16}$$

This relation fixes the sum

$$\kappa_- + \kappa_+ = (v_c/\sqrt{K_c})\,\partial v_s/\partial\mu. \tag{17}$$

Moreover, Galilean invariance requires that the charge current and momentum operators for model in Eqs. (7) and (13) be proportional to each other.[5] The momentum operator is obtained from the energy-momentum tensor; its density is

$$\mathcal{P} = \frac{2k_F}{\sqrt{K_c}}(J_R - J_L) + 2\pi(J^2_R - J^2_L) + \frac{2\pi}{3}(\mathbf{J}^2_R - \mathbf{J}^2_L). \tag{18}$$

The current density $\mathcal{J}(x)$ is obtained from the continuity equation for the charge density

$$\partial_t n(x) = -i\int dx'[n(x), \mathcal{H}_\ell(x') + \delta\mathcal{H}(x')] = -\partial_x\mathcal{J}(x). \tag{19}$$

We then impose the condition $\mathcal{J}(x) = \mathcal{P}(x)/m$ for a Galilean-invariant system. The relation between the coefficients of the spin contributions to $\mathcal{P}(x)$ and $\mathcal{J}(x)$ leads to

$$\kappa_- - \kappa_+ = 1/(\sqrt{K_c}m). \tag{20}$$

Equations (17) and (20) allow one to determine $\kappa_\pm$ by simply measuring the spin dispersion at low energies.

Finally, the coefficient κ_3 is related to the variation in the backscattering coupling constant $v_s g$ under a change of the chemical potential

$$\kappa_3 = -\frac{3v_c}{2\sqrt{K_c}}\frac{\partial(v_s g)}{\partial\mu}. \tag{21}$$

Since g is marginally irrelevant, we expect κ_3 to be more irrelevant than the other coupling constants in Eq. (13), in the sense of logarithmic corrections to scaling. This will be discussed in the following section.

Renormalization-group flow with irrelevant operators

All the operators in Eq. (13) are irrelevant and have the same scaling dimension $x=3$. The renormalization-group (RG) equations for the irrelevant coupling constants [including the marginal g term in Eq. (7)] can be derived by integrating out high-energy modes in the partition function as one lowers the ultraviolet momentum cutoff Λ. Following the notation of Ref. 19, we rescale the coupling constants by the cutoff and introduce $\tilde{\eta}_\pm = \Lambda\eta_\pm$, $\tilde{\kappa}_\pm = \Lambda\kappa_\pm$, and $\tilde{\kappa}_3 = \Lambda\kappa_3$. To obtain the quantum corrections to scaling, we use the operator product expansion (OPE) of the spin currents[1]

$$\begin{aligned}:J^a_L(z) :: J^b_L(0): &\sim \frac{\delta^{ab}}{8\pi^2 z^2} + \frac{i\varepsilon^{abc}}{2\pi z}:J^c_L(0):, \\ :J^a_R(\bar{z}) :: J^b_R(0): &\sim \frac{\delta^{ab}}{8\pi^2 \bar{z}^2} + \frac{i\varepsilon^{abc}}{2\pi \bar{z}}:J^c_R(0):,\end{aligned} \tag{22}$$

where $z = v_s\tau + ix$ and $\bar{z} = v_s\tau - ix$, with τ the imaginary time, and ε^{abc} is the Levi-Civita antisymmetric tensor. [The normal ordering symbol :: is implicit in the Hamiltonians (7) and (13).] The OPE for the scalar currents is simply

$$\begin{aligned}:J_L(x,\tau) :: J_L(0,0): &\sim \frac{1}{8\pi^2(v_c\tau + ix)^2} + \cdots, \\ :J_R(x,\tau) :: J_R(0,0): &\sim \frac{1}{8\pi^2(v_c\tau - ix)^2} + \cdots.\end{aligned} \tag{23}$$

We integrate out high-energy modes in the shell $1/\Lambda < |z| < 1/\Lambda'$ with $\Lambda' = \Lambda e^{-d\ell}$, $d\ell \ll 1$. This choice of cutoff is

rotationally invariant for the spin modes but elliptical for the charge modes. In order to get a nonzero contribution to the RG equation after integrating out the shell in the (x,τ) plane, it is important to contract both right and left movers at the same time.

In the presence of the dimension-three operators, the velocities, Luttinger parameter and chemical potential are renormalized, but flow to their fixed-point values in the low-energy limit. This flow is already taken into account if we use the exact parameters. The interesting RG flow here is given by the coupled equations for $\tilde{\kappa}_3$ and g

$$\frac{dg}{d\ell} = -g^2, \tag{24}$$

$$\frac{d\tilde{\kappa}_3}{d\ell} = -(1+2g)\tilde{\kappa}_3. \tag{25}$$

There are no corrections to the scaling of $\tilde{\eta}_\pm$ and $\tilde{\kappa}_\pm$ to second order in the coupling constants. Equation (25) can be rewritten as

$$\frac{d\kappa_3}{d\ell} = -2g\kappa_3. \tag{26}$$

On the right-hand side of Eqs. (24) and (26) we have terms of zeroth order in Λ. It follows that

$$\frac{d\ln g}{d\ell} = -g = \frac{1}{2}\frac{d\ln \kappa_3}{d\ell}. \tag{27}$$

The solution is of the form

$$\kappa_3(\ell)/[g(\ell)]^2 = \text{const}. \tag{28}$$

The scaling of the marginal coupling constant is the familiar one

$$g(\Lambda) = \frac{g}{1+g\ln(\Lambda_0/\Lambda)}, \tag{29}$$

where Λ_0 is the initial value of the cutoff. As a result, for positive $g \ll 1$ and for $\Lambda \ll \Lambda_0 e^{-1/g}$ the effective $g(\Lambda)$ vanishes logarithmically as $g(\Lambda) \sim 1/\ln(\Lambda_0/\Lambda)$. If the bare g at high energies is of order 1, the perturbative result in Eq. (29) is still valid if g is interpreted as $g(\Lambda_0)$ at some scale $\Lambda_0 \ll k_F$ such that $g(\Lambda_0) \ll 1$. In any case, we obtain $g(\Lambda) \sim 1/\ln(\Lambda_0/\Lambda)$ in the low-energy limit.

More interestingly, Eq. (28) implies

$$\kappa_3(\Lambda) = \frac{\kappa_3}{[1+g\ln(\Lambda_0/\Lambda)]^2}. \tag{30}$$

Therefore, $\kappa_3(\Lambda)$ vanishes as $\kappa_3(\Lambda) \sim 1/\ln^2(\Lambda_0/\Lambda)$ as $\Lambda \to 0$. This will be important in Sec. IV D when we compare leading logarithmic corrections to the DCSF due to g and κ_3.

IV. DYNAMICAL CHARGE STRUCTURE FACTOR

In the bosonized form of Eq. (8), the DCSF is given by

$$S(q,\omega) = -8K_c \,\mathrm{Im}\, C^{\mathrm{ret}}(q,\omega), \tag{31}$$

where $C^{\mathrm{ret}}(q,\omega)$ is the retarded correlation function for the charge current J_R+J_L, which can be obtained by analytic continuation from the Matsubara correlation function

$$C(q,i\omega) = \sum_{\alpha,\beta=R/L} C_{\alpha\beta}(q,i\omega), \tag{32}$$

$$C_{\alpha\beta}(q,i\omega) = -\int_0^L dx e^{-iqx}\int_0^\beta d\tau e^{i\omega\tau} \times \langle J_\alpha(x,\tau)J_\beta(0,0)\rangle. \tag{33}$$

Equation (33) involves the charge boson propagator. Within the Luttinger model, the charge boson is free and we have $C^0_{LL}=C_L$, $C^0_{RR}=C_R$, and $C^0_{LR}=C^0_{RL}=0$ with

$$C_{R/L}(x,\tau) \equiv \langle J_{R/L}(x,\tau)J_{R/L}(0,0)\rangle = \frac{1}{8\pi^2}\frac{1}{(v_c\tau \mp ix)^2}. \tag{34}$$

Taking the Fourier transform, we obtain

$$C_{R/L}(q,i\omega) = \frac{1}{4\pi}\frac{\pm q}{i\omega \mp v_c q}. \tag{35}$$

As a result, the DCSF calculated in the linear dispersion approximation is given by

$$S(q,\omega) = 2K_c q\,\delta(\omega - v_c q). \tag{36}$$

That the DCSF is given by a delta-function peak at the energy of the free charge boson follows from spin-charge separation and Lorentz invariance of the Luttinger model. This should be contrasted with the free-electron result in Eq. (5), where the peak associated with particle-hole excitations has a q^2 broadening due to the curvature of the dispersion about the Fermi points.

A. Width of the charge peak

We can calculate $S(q,\omega)$ beyond the Luttinger liquid result by analyzing the effects of the boson-boson interactions in Eq. (13). First, let us consider the broadening of the charge peak. The charge-only $\eta_\pm$ terms are familiar from the spinless case.[12] They account for the decay of one charge boson into two charge bosons. In particular, η_- is a three-leg vertex in which one right- (left-) moving boson decays into two right- (left-) moving bosons, thus coupling the single-boson state to degenerate multiboson states. It is known that perturbation theory in η_- is badly divergent but can be dealt with by refermionization.[7,11] Near the charge mass shell, $\omega \approx v_c q$, we introduce a spinless *holon* field $\psi_{c,R}$ such that $\psi^\dagger_{c,R}\psi_{c,R} = \sqrt{2}J_R$. The η_- term in Eq. (13) then maps onto a parabolic dispersion about the holon Fermi point

$$\frac{4\pi^2}{3}\eta_- J_R^3 \to -\frac{\eta_-}{2\sqrt{2}}\psi^\dagger_{c,R}\partial_x^2\psi_{c,R}. \tag{37}$$

It can be argued that η_- determines the exact broadening of the DCSF to order q^2 because it gives rise to the bosonic diagrams that are most singular at $\omega = v_c q$.[12] Within the approximation of neglecting the other dimension-three operators, the charge sector of the Luttinger model plus the η_- term refermionizes into a free fermion model with dispersion

$\epsilon_c(k) \approx v_c k + \eta_- k^2/(2\sqrt{2})$, for k measured from the right Fermi point. The support of the charge peak in the DCSF is then given by the spectrum of excitations with a single holon-antiholon pair. Due to the curvature of the dispersion, these excitations define a continuum bounded by

$$\omega_{c\pm}(q) = v_c q \pm \eta_- q^2/2\sqrt{2}. \tag{38}$$

Therefore, at order q^2, the charge peak has a free-fermionlike line shape

$$S(q,\omega) \approx \frac{2\sqrt{2}K_c}{\eta_- q}\theta\left(\frac{\eta_- q^2}{2\sqrt{2}} - |\omega - v_c q|\right). \tag{39}$$

The parameter $\sqrt{2}/\eta_-$ can be interpreted as a renormalized holon mass.

It is interesting that the limits $q \to 0$ and $\tilde{V}_0 \to 0$ in the width do not commute. For $q \ll m\tilde{V}_0 \ll k_F$, we have from Eq. (14) that $\delta\omega_c(q) = \eta_- q^2/\sqrt{2} \approx q^2/(\sqrt{2}m)$. The $\sqrt{2}$ factor makes the charge peak narrower than the free electron result in Eq. (5).[20] In particular, this means that in the regime $q \ll m\tilde{V}_0$ the holon dispersion (which shows up, for instance, in the single-electron spectral function) should not be regarded as a smooth continuation of the electron dispersion. An important crossover happens at $q \sim m\tilde{V}_0$.

The result in Eq. (38) can be directly compared with the exact width of the two-holon continuum for an integrable model, such as the Yang-Gaudin model.[21] We have numerically solved the standard Bethe ansatz integral equations for the spectrum of elementary excitations of the Yang-Gaudin model. We verified that the width defined as the difference between the maximum and minimum exact energies of a particle-hole excitation in the holon Fermi sea for momentum $q \ll m(v_c - v_s)$ agrees with Eq. (38), including the factor of $\sqrt{2}$ and with η_- calculated from the phenomenological relation in Eq. (14).

Corrections to Eq. (39) due to residual holon-holon interactions are higher order in q. These corrections include a high frequency tail at order η_+^2, analogous to the spinless case,[10,12,18] and possible asymmetries of the charge peak near the edges of the two-holon continuum, due to x-ray edge-type singularities.[16] But before we discuss the behavior near $\omega_{c\pm}(q)$, we turn to the contributions from the spin operators in Eq. (13).

B. Spin peak

The $\kappa_\pm$ operators in Eq. (13) allow for decay of the charge boson into two spin bosons moving in the same direction and carrying the total energy $\omega \approx v_s q$. The corresponding three-leg vertices are illustrated in Fig. 1. As noted in Ref. 18, this process gives rise to a narrow peak in the DCSF centered at $\omega = v_s q$ which corresponds to a charge-carrying spin singlet excitation. Let us calculate the correction to the charge boson propagator in Eq. (33) using second-order perturbation theory in $\kappa_\pm$. For instance, the $\mathcal{O}(\kappa_-^2)$ correction to C_{RR} is

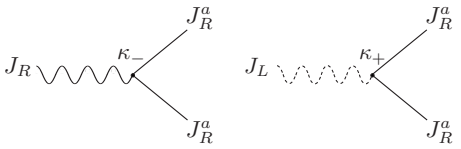

FIG. 1. Decay of a charge boson (propagators denoted by wiggly lines) into two right-moving spin bosons (propagators denoted by straight lines). This process leads to a spin peak in the dynamic charge-structure factor.

$$\delta C_{RR}^{\kappa_-}(q,i\omega) = 32\pi^4\kappa_-^2[C_R(q,i\omega)]^2\Pi_{RR}(q,i\omega), \tag{40}$$

where we made use of the identity: $\mathbf{J}_{R/L}^2 := 3(J_{R/L}^z)^2$ and introduced the boson self-energy

$$\Pi_{\alpha\beta}(q,i\omega) = -\int dx e^{-iqx}\int_0^\beta d\tau e^{i\omega\tau} S_\alpha(x,\tau)S_\beta(x,\tau). \tag{41}$$

Here S_α, $\alpha = R,L$, are the free chiral spin boson propagators

$$\delta^{ab}S_{R/L}(x,\tau) = \langle J_{R/L}^a(x,\tau)J_{R/L}^b(0,0)\rangle = \frac{\delta^{ab}}{8\pi^2}\frac{1}{(v_s\tau \mp ix)^2}. \tag{42}$$

In momentum and frequency space, we have

$$S_{R/L}(q,i\omega) = \frac{1}{4\pi}\frac{\pm q}{i\omega \mp v_s q}. \tag{43}$$

We then calculate Π_{RR} that appears in Eq. (40)

$$\begin{aligned}(4\pi)^2\Pi_{RR}(q,i\omega) &= -\int_0^\infty \frac{dq'}{2\pi}\int_{-\infty}^\infty \frac{d\omega'}{2\pi}\frac{q'}{i\omega' - v_s q'} \\ &\quad\times \frac{q-q'}{i\omega - i\omega' - v_s q + v_s q'} \\ &= \frac{q^3}{12\pi}\frac{1}{i\omega - v_s q}.\end{aligned} \tag{44}$$

Adding up all second-order contributions from κ_- and κ_+ and taking the imaginary part of the retarded self-energy, we obtain[18]

$$\delta S(q,\omega) \approx (K_c/12)(\alpha_- + \alpha_+)^2 q^3 \delta(\omega - v_s q), \tag{45}$$

where

$$\alpha_\pm = \kappa_\pm/(v_c \pm v_s). \tag{46}$$

This shows that the DCSF exhibits a narrow peak with spectral weight of order q^3 at the spin mass shell $\omega = v_s q$.

The question then is how the spin peak in Eq. (45) is broadened by treating band curvature operators to higher orders. We first note that the condition $q \ll m(v_c - v_s)$ ensures that the spin peak is well separated from the charge peak. By analogy with the discussion in Sec. IV A, we expect that the width of the spin peak is set by decay processes that couple degenerate states with multiple spin bosons propagating in the same direction. However, in contrast with the case of the charge peak, in Eq. (13) there is no dimension-three spin-only chiral operator that would be equivalent to a parabolic dispersion about spinon Fermi points. Thus the broadening

of the spin peak must come from higher-order on-shell decay processes. In fact, the leading irrelevant spin-boson interactions allowed by symmetry are *quartic* in the spin currents

$$\zeta_-(\mathbf{J}_{R/L}^2)^2, \zeta_+\mathbf{J}_R^2\mathbf{J}_L^2, \lambda_1(\mathbf{J}_R\cdot\mathbf{J}_L)^2, \lambda_2\mathbf{J}_R\cdot\mathbf{J}_L(\mathbf{J}_R^2+\mathbf{J}_L^2). \quad (47)$$

In principle, these operators are present as perturbations to model in Eq. (7) plus Eq. (13). They are also generated by "projecting" into a subspace with energy $|\omega - v_s q| \ll (v_c - v_s)q$ and integrating out "high-energy" charge bosons. The spin part of the resulting model for $\omega \approx v_s q$ is equivalent to the low-energy effective model for the XXZ spin chain at zero magnetic field.[22]

Perturbation theory in the dimension-four operators in Eq. (47) is highly singular for $\omega \approx v_s q$.[12] Unfortunately, it is not known how to sum up the expansion in this case. Refermionization does not solve the problem because the effective fermionic model with dimension-four operators contains not only band curvature terms, such as $\psi^\dagger\partial_x^3\psi$, but also *intrabranch* (i.e., which do not mix R and L) residual interactions of the form $\psi^\dagger\partial_x\psi\partial_x\psi^\dagger\psi$, which also contribute to the broadening at leading order in q. Nevertheless, simple power counting tells us that the width of the spin peak should scale like $\delta\omega_s(q)\sim\mathcal{O}(q^3)$, rather than $\mathcal{O}(q^2)$. This is consistent with the result for the DSSF of the XXZ model at zero field,[12] where it is known that the spectral weight is dominated by two-spinon excitations and the exact spinon dispersion takes the form $\epsilon_s(k)=v_s\sin(k)\approx v_s(k-k^3/6+\cdots)$ about the spinon Fermi points.

C. Edge singularities of the spin peak

To be able to say more about the line shape of the spin peak, we refermionize the spin currents into *interacting* spinless fermions. This is equivalent to inverting the Jordan-Wigner transformation in the continuum and writing down a SU(2) symmetric model for the fermions associated with the spin excitations. In other words, the idea is analogous to deriving the bosonic Hamiltonian for the Heisenberg spin chain by starting from the XXZ model and tuning the Luttinger parameter to the SU(2) symmetric value (a strongly interacting limit with Luttinger parameter $K=1/2$), as opposed to deriving the bosonic Hamiltonian directly from the Hubbard model (in which case the spin bosons come out noninteracting with $K_s=1$).[1,23] The new ingredient here is that the spin excitations are coupled to gapless charge modes.

The mapping of the bare chiral fermion densities to the spin currents in Eq. (7) is $\psi_{s,R/L}^\dagger\psi_{s,R/L}=(3J_{R/L}^z-J_{L/R}^z)/2$, as follows from a canonical transformation for the spin bosonic fields. Spin inversion symmetry implies that the dispersion of these fermionic spinons is particle-hole symmetric. We assume that the exact dispersion about the right Fermi point is given by

$$\epsilon_s(k) \approx v_s k - \gamma k^3 \quad (48)$$

with the unknown parameter $\gamma>0$. We expect that γ stems from dimension-four operators in the bosonic model and is of order $1/(mk_F)$.

In terms of fermions, the operator $\mathbf{J}_R^2$ that gives rise to the spin peak in Eq. (45) creates particle-hole pairs on the spinon Fermi sea. We can study the behavior near the edges of multispinon continua using the methods of Refs. 16 and 24. The absolute lower threshold $\omega_{s-}(q)=\epsilon_s(q)$ is defined by an excitation with a particle at the Fermi surface and a hole at momentum $-q$ below the Fermi point. For $\omega-\omega_{s-}(q)\ll\gamma q^3$, we define a "deep spinon" subband by expanding[16]

$$\psi_{sR} \sim \psi_{sr} + e^{-iqx}d_s^\dagger, \quad (49)$$

where $\psi_{sr}^\dagger$ creates low-energy spinons near the right Fermi point and $d_s^\dagger$ creates a hole at momentum $-q$ below the Fermi point. This leads to the quantum impurity model

$$\mathcal{H}_s^- = \mathcal{H}_\ell + d_s^\dagger(\omega_{s-} - iu\partial_x)d_s - (V_r J_r^z + V_l J_l^z)d_s^\dagger d_s + 2\pi q(\kappa_-' J_r + \kappa_+' J_l)d_s^\dagger d_s, \quad (50)$$

where $u\approx v_s - 3\gamma q^2$ is the velocity of the d_s hole. The spin-only part of the quantum impurity model given by the first line in Eq. (50) is derived as explained in Ref. 24, by applying the mode expansion in Eq. (49) to a generic model of interacting spinless fermions with the dispersion in Eq. (48). The second line stems from the coupling of the energy density of the spinon field to the bosonized holon density. Here $J_{r/l}$ stand for the bosonized charge currents with cutoff at energy scale $\ll\gamma q^3$, which allows the "high-energy" spinon to emit low-energy charge bosons such that the energy remains near $\omega=\omega_{s-}(q)$. Note that in this procedure we keep only *marginal* operators in the quantum impurity model, as irrelevant operators can only introduce subleading power-law singularities at the threshold. This is not to be confused with the presence of irrelevant operators in the original bosonic model in Eq. (13), which are essential to argue for the nonlinearity of holon and spinon dispersions and for the very existence of the deep spinon threshold.

Rather than keep track of the parameters in the derivation of model in Eq. (50), it is more useful to introduce the model phenomenologically (it contains all the marginal operators allowed by symmetry) and to fix the coupling constants by symmetry and phenomenological relations. The parameters $V_{r/l}$ can be fixed by realizing that the same model in Eq. (50) can be used to calculate the lower edge singularity of the DSSF. This is because the operator $J_{R/L}^z$ that enters the longitudinal spin-spin correlation function also creates two-spinon excitations in the fermionic representation, and the lower threshold of the support of the DSSF is also given by the deep spinon excitation. The important constraint comes from SU(2) symmetry, which imposes that the exponents for the longitudinal and transverse DSSF must coincide.[25] We reproduce this argument in detail in the Appendix.

The coupling constants $\kappa_\pm'$ in Eq. (50) are related to exact phase shifts at the holon Fermi points due to the creation of a high-energy spinon. We want to show that at small q these are also related to the band curvature parameters in Eq. (13). It is easy to show that an infinitesimal change in the chemical potential $\delta\mu$ gives rise to a shift in the energy of the high-energy spinon $\delta\omega_{s-}=\delta\mu\sqrt{K_c}(\kappa_-'+\kappa_+')q/v_c$. This allows us to write

$$\kappa_-' + \kappa_+' = \frac{v_c}{\sqrt{K_c}q}\frac{\partial \omega_{s-}}{\partial \mu}. \tag{51}$$

But from the exact spinon dispersion we have $\omega_{s-}=v_s q + \mathcal{O}(q^3)$, hence

$$\kappa_-' + \kappa_+' = \frac{v_c}{\sqrt{K_c}}\frac{\partial v_s}{\partial \mu} + \mathcal{O}(q^2). \tag{52}$$

The second relation for $\kappa_-' - \kappa_+'$ can be obtained by imposing Galilean invariance to Hamiltonian (50). Similarly to the discussion in Sec. III, we compare momentum and current operators. The contribution from the spin-charge coupling terms in Eq. (50) to the current density (defined from the continuity equation for the charge density) is

$$\mathcal{J}_d = \sqrt{K_c}q(\kappa_-' - \kappa_+')d_s^\dagger d_s. \tag{53}$$

Therefore, if we consider an excited state in which we create a particle-hole pair of spinons with a deep hole at momentum $k_F - q$ and a particle at k_F, the current of this state is $\sqrt{K_c}q(\kappa_-' - \kappa_+')$. Demanding that this current be equal to the momentum q of the state divided by the mass m, we find

$$\kappa_-' - \kappa_+' = 1/(\sqrt{K_c}m). \tag{54}$$

Comparing Eqs. (52) and (54) with Eqs. (17) and (20), we conclude that

$$\kappa_\pm' = \kappa_\pm + \mathcal{O}(q^2). \tag{55}$$

Using the model in Eqs. (50) and (55), we can show (see Appendix) that the DCSF diverges at the lower edge of the two-spinon continuum as $S(q,\omega)\sim(\omega-\omega_{s-})^{\mu_{s-}}$ with exponent

$$\mu_{s-} = -1/2 + (\alpha_-^2 + \alpha_+^2)q^2/2 + \mathcal{O}(q^4), \tag{56}$$

where $\alpha_\pm$ is defined in Eq. (46). Therefore, as $q\to 0$, the exponent approaches the universal value $-1/2$, which depends only on SU(2) symmetry. The q^2 correction to μ_{s-} is due to the coupling to gapless charge bosons with energy $\ll \gamma q^3$. This exponent should be contrasted with the square-root singularity of the DSSF for the Heisenberg model.[26] We note that μ_{s-} differs from the corresponding exponent for SU(2) bosons at the magnon threshold, $\mu_m=-1+\mathcal{O}(q^2)$.[27,28]

The upper edge of the two-spinon continuum is given by $\omega_{s+}(q)=2\epsilon_s(q/2)$. As discussed in Ref. 24, near this edge the spectral weight is suppressed by resonant scattering between spinons with equal velocity. If most of the spectral weight of the spin peak is due to two-spinon excitations, the width can be defined as

$$\delta\omega_s(q) = \omega_{s+}(q) - \omega_{s-}(q) = 3\gamma q^3/4. \tag{57}$$

While the upper threshold of two-spinon continuum in the integrable XXZ model exhibits a square-root cusp, here we expect that the upper threshold of the two-spinon continuum is rounded by higher order (in q) processes, at least for non-integrable models.

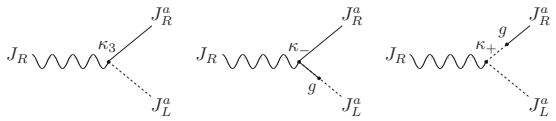

FIG. 2. Processes that contribute to the effective vertex $\kappa_3^{\rm eff}$ in Eq. (59) to leading order in dimension-three operators. The decay of the charge boson into a pair of right- and left-moving spin bosons leads to a tail in the charge-structure factor for $\omega > v_s q$.

D. Smearing of the charge peak: decay rate of the charge boson

In general, we expect $S(q,\omega)$ to have nonzero spectral weight anywhere above the lower threshold $\omega_{s-}(q)$. A tail between the spin and charge peaks is generated due to the decay of the charge boson into a pair of L and R spin bosons, as depicted in Fig. 2. The effective vertex is calculated from the three-point function

$$\begin{aligned} G(\mathbf{k}_1,\mathbf{k}_2,\mathbf{k}_3) &\equiv \langle (J_L + J_R)(\mathbf{k}_1) J_L^a(\mathbf{k}_2) J_R^b(\mathbf{k}_3)\rangle \\ &= \frac{4\pi^2}{3}\kappa_3^{\rm eff}\delta^{ab}(C_L + C_R)(\mathbf{k}_1)S_L(\mathbf{k}_2)\times S_R(\mathbf{k}_3) \\ &\quad \times (2\pi)^2\delta(\mathbf{k}_1+\mathbf{k}_2+\mathbf{k}_3), \end{aligned} \tag{58}$$

where $\mathbf{k}=(k,\omega)$ is a two-momentum. To first order in $\kappa_\pm, \kappa_3$ [leading order in q/k_F in the contribution to $S(q,\omega)$], there are two contributions to the effective vertex, one from κ_3 and the other from a combination of $\kappa_\pm$ and g. We find

$$\kappa_3^{\rm eff} = \kappa_3 + \frac{3}{2}g(\kappa_- + \kappa_+). \tag{59}$$

Away from the spin and charge mass shells, i.e., for $|\omega - v_s q| \gg \delta\omega_s(q)$ and $|\omega - v_c q| \gg \delta\omega_c(q)$, the tail of the spin peak can be calculated by second-order perturbation theory in $\kappa_3^{\rm eff}$. Similarly to the calculation in Sec. IV B, we obtain a correction to the charge boson propagators

$$\delta C_{\alpha\beta}^{\kappa_3^{\rm eff}}(q,i\omega) = -\frac{16\pi^4}{3}(\kappa_3^{\rm eff})^2 C_\alpha(q,i\omega)C_\beta(q,i\omega)\Pi_{RL}(q,i\omega), \tag{60}$$

where $\alpha,\beta=R,L$ and $\Pi_{RL}(q,i\omega)$ is the self-energy with one right-moving and one left-moving spin boson, as defined in Eq. (41). The calculation of Π_{RL} yields[12]

$$\begin{aligned} \Pi_{RL}^{\rm ret}(q,\omega) = \frac{1}{32\pi^3}\Bigg[&\frac{\Lambda^2}{2v_s} - \frac{\omega^2 - v_s^2 q^2}{8v_s^3} \\ &\times \log\frac{(v_s q)^2 - (\omega + i\eta)^2}{4v_s^2\Lambda^2}\Bigg]. \end{aligned} \tag{61}$$

While the real part is ultraviolet divergent, the imaginary part is not. The imaginary part gives the tail in the DCSF

$$\delta S(q,\omega) \approx \frac{K_c(\kappa_3^{\rm eff})^2}{24 v_s^3}\left[\frac{v_c q^2}{\omega^2 - v_c^2 q^2}\right]^2(\omega^2 - v_s^2 q^2) \tag{62}$$

for $\omega > v_s q$ and $|\omega - v_c q| \gg \eta_- q^2$.

At this point, we recall that both g and κ_3 that appear in the amplitude for $\kappa_3^{\rm eff}$ scale logarithmically with the infrared

cutoff (see Sec. III). Within RG improved perturbation theory, the bare g and κ_3 in Eq. (59) are replaced by the renormalized ones in Eqs. (29) and (30), with cutoff set by the small momentum $\Lambda \sim q$. In the long-wavelength limit, such that $g(q) \sim 1/\ln(k_F/q) \ll 1$, we have

$$g(q) \sim 1/\ln(k_F/q), \tag{63}$$

$$\kappa_3(q) \sim (\kappa_3/g^2)/\ln^2(k_F/q). \tag{64}$$

At leading logarithmic order, we can drop the contribution from κ_3 in $\kappa_3^{\text{eff}}(q)$ and Eq. (62) becomes

$$\delta S(q,\omega) \approx \frac{3K_c[g(q)]^2}{32v_s^3}\left[\frac{v_c(\kappa_- + \kappa_+)q^2}{\omega^2 - v_c^2q^2}\right]^2(\omega^2 - v_s^2q^2). \tag{65}$$

The DCSF was calculated by similar methods in Ref. 18 but the tail between the spin and charge peaks was not obtained because backscattering processes (g and κ_3 in our notation) were neglected.

The presence of the tail means that the charge peak discussed in Sec. IV A is inside a continuum of spin excitations. The coupling to the continuum results in a decay rate for the charge excitations. The imaginary part of the self-energy Π_{RL} can be absorbed into the charge boson propagator in the form

$$C_{R/L}^{\text{ret}}(q,\omega) = \frac{1}{4\pi}\frac{\pm q}{\omega \mp v_c q + i/\tau_c}, \tag{66}$$

where $\tau_c^{-1}(q)$ is the decay rate given by

$$\frac{1}{\tau_c} = \frac{\pi(\kappa_3^{\text{eff}})^2(v_c^2 - v_s^2)q^3}{192v_s^3}. \tag{67}$$

In the limit $g(q) \sim 1/\ln(k_F/q) \ll 1$, we obtain

$$\frac{1}{\tau_c} = \frac{3[g(q)]^2\pi(\kappa_- + \kappa_+)^2(v_c^2 - v_s^2)q^3}{256v_s^3}. \tag{68}$$

For $q \ll m(v_c - v_s)$, the decay rate in Eq. (68) is smaller than $\delta\omega_c(q) \sim q^2$, which is due to decay of the charge boson within the charge sector (see Sec. IV A). However, τ_c^{-1} is important because it is responsible for rounding off the edges of the charge peak. This can be confirmed by calculating the decay rate for a single high-energy holon—a d_c particle in the quantum impurity model for the edges of the two-holon continuum, similar to the calculation in Ref. 29 for the spinless case. The decay rate is due to the perturbation

$$\delta\mathcal{H}_3 \sim \xi_3 d_c^\dagger d_c \partial_x \varphi_R^s \partial_x \varphi_L^s. \tag{69}$$

The parameter ξ_3 gives the amplitude for a process in which a holon scatters off two spinons moving in opposite direction. This is *not* a three-electron scattering process and, in principle, $\xi_3 \neq 0$ even for integrable models. Using the result in Eq. (5.8) of Ref. 29, we obtain

$$\frac{1}{\tau_c} \propto \frac{(\xi_3)^2(v_c^2 - v_s^2)[\Lambda(q)]^3}{v_c^3}, \tag{70}$$

where $\Lambda(q)$ is the cutoff of the high-energy subband. Setting $\Lambda(q) \sim q$, we recover the momentum and interaction dependence of the decay rate in Eq. (68) if we assume that ξ_3 does not vanish as a power law of q in the limit $q \to 0$. From comparison with Eq. (67), we expect $\xi_3 \propto \kappa_3^{\text{eff}}$. This should be contrasted with the spinless case, where the coupling constant in Eq. (5.13) of Ref. 29 has to vanish like q^2 because of statistics, since there is no s-wave scattering for spinless fermions. For the spinful case, statistics alone does not imply that the amplitude ξ_3 vanishes as q^2 or high powers of q.

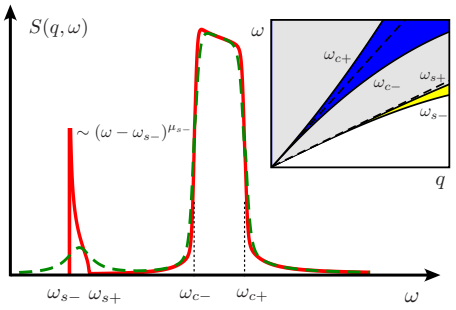

FIG. 3. (Color online) Schematic excitation spectrum (inset on the upper right corner) and line shape (main figure) for the DCSF of spin-1/2 fermions at small q. The dashed lines in the (q,ω) plane represent the linear dispersion of charge and spin modes in the Luttinger model. The two-holon and two-spinon continua are represented by blue and yellow regions bounded by $\omega_{c\pm}(q)$ and $\omega_{s\pm}(q)$, respectively. At zero temperature and in the regime $q \ll m(v_c - v_s)$, the line shape of $S(q,\omega)$ (solid red line in the main figure) has well defined peaks inside the two-holon and two-spinon continua. At finite temperature $\delta\omega_s(q) \ll g^2T \ll v_c q$, diffusion broadens the spin peak into a Lorentzian (dashed green line).

Note also that the result for $1/\tau_c$ in Eq. (68) is nonperturbative in the electron-electron interaction, since for $q \ll m\tilde{V}_0 \ll k_F$, we have $\tau_c^{-1} \sim g^2\tilde{V}_0 q^3/k_F^2$, which is *third* order in the interaction strength. Furthermore, this result implies that, even for an integrable model, the power-law singularities[16] at $\omega_{c\pm}$ are removed at order q^3. The same decay rate $1/\tau_c$ rounds off the singularity at the holon mass shell in the electron spectral function.[30] This is remarkably different from the spinless case, where it is believed that integrable models can have exact singularities above the lower threshold because the decay rate of a high-energy particle may vanish exactly.[29]

We note that if the phenomenological relations Eqs. (17) and (21) are valid for the running coupling constants and we substitute them in Eq. (59), we find

$$\kappa_3^{\text{eff}} = -(3/2)v_c v_s K_c^{-1/2}\,\partial g/\partial\mu. \tag{71}$$

At low energies, $g(\Lambda) \sim g(\Lambda_0)/[1 + g(\Lambda_0)\ln(\Lambda_0/\Lambda)]$. It is not clear how imposing the phenomenological relations at all energy scales can be reconciled with the result from the RG. It is important for our results in Eqs. (65) and (68) that even if $\partial g/\partial\mu = 0$ at some energy scale, the effective vertex κ_3^{eff} will be generated by the RG flow because κ_3 and g scale differently, and the leading logarithmic dependence is due to the g term in Eq. (59).

Finally, putting together all the pieces, we construct the final picture for the DCSF at zero temperature in Fig. 3. Note, in particular, that there is only a rounded threshold at $\omega \approx \omega_{c-}$.

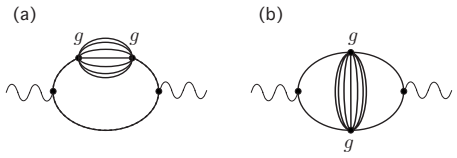

FIG. 4. Diagrams at $\mathcal{O}(\kappa_{\pm}^2 g^2)$ in the self-energy for the charge boson: (a) self-energy correction to the spin boson propagator and (b) vertex correction. The bubble with multiple lines denotes the correlation function for the operator $J_R^+ J_L^- \sim e^{i\sqrt{4\pi}(\varphi_R^s - \varphi_L^s)}$, following Ref. 33.

E. Finite-temperature effects

We now discuss the effects of finite temperature on the broadening of the charge and spin peaks in the DCSF. This will be important to compute the temperature dependence of the drag resistivity in Eq. (1).

We consider the regime where both temperature and band curvature energy scale are small compared to the scale of spin-charge separation: $T \ll (v_c - v_s) v_c / \eta_-$ and $q \ll (v_c - v_s)/\eta_-$. Assuming that v_c, v_s, and $v_c - v_s$ are all on the order of v_F and $1/\eta_-$ is on the order of m, these conditions mean roughly $T \ll T_F = m v_F^2/2$ and $q \ll k_F$. This is the regime in which we may expect the spin and charge peaks to remain well separated. Neglecting the overlap between the spin and charge peaks, the line shape of the charge peak can be approximated by the finite temperature result for the imaginary part of the density-density correlation function for free fermions with mass $\sqrt{2}/\eta_-$ (Refs. 10 and 17)

$$A(q,\omega,T) \approx \frac{\sqrt{2}K_c}{\eta_- q}[n_F(w_+) - n_F(w_-)], \tag{72}$$

where $n_F(\omega) = 1/(1+e^{\omega/T})$ is the Fermi-Dirac distribution function and $w_\pm \equiv [(\omega \pm \delta\omega_c/2)^2 - (v_c q)^2]/(2\delta\omega_c)$, with $\delta\omega_c = \delta\omega_c(q) = \eta_- q^2/\sqrt{2}$. The width of the charge peak at finite temperature is then of the order of $\max\{\eta_- q^2, \eta_- q T/v_c\}$.

The calculation of the width of the spin peak is more complicated because we do not have an approximation in terms of noninteracting spinless fermions. For the purpose of calculating the drag resistivity in Eq. (1), we are only interested in whether for fixed small q and at low temperature the spin peak can become broader than the charge peak. On the one hand, the broadening due solely to band curvature must be of order $(\gamma q^2/v_s)T$ for $T \sim v_s q$. As long as $q, T/v_s \ll m(v_c - v_s), \eta_-/\gamma$, this is small compared to the broadening of charge peak. On the other hand, thermal effects have a stronger effect on spin excitations because the latter are damped by diffusion.[31,32]

Recall that the spin peak stems from the self-energy with two spin bosons propagating in the same direction (see Fig. 1). We can calculate the finite-temperature broadening by neglecting band curvature operators and applying perturbation theory in the marginally irrelevant operator g in Eq. (7). As we did in Sec. IV D, we neglect the κ_3 vertex in the leading logarithmic approximation. To order $(\kappa_\pm g)^2$, there are two types of diagrams in the self-energy for the charge boson, as illustrated in Fig. 4. The first type amounts to a self-energy correction to the spin boson propagator. The transverse part of the perturbation, $-\pi v_s g(J_L^+ J_R^- + \text{H.c.})$ gives rise to a nonzero imaginary part of the retarded self-energy, which can be calculated following Ref. 33. We can sum up the series for this type of diagram by defining the dressed spin propagator

$$\tilde{S}_R(q, i\omega) = \frac{1}{4\pi} \frac{q}{i\omega - v_s q - \Sigma(q, i\omega, T)}. \tag{73}$$

The other type of diagram [Fig. 4(b)] is a vertex correction. Since the thermal broadening of the spin peak is already obtained within the approximation of keeping only self-energy-type diagrams such as the one in Fig. 4(a), we will make the approximation of neglecting vertex corrections. By doing this, the two-spin-boson correlation function becomes

$$\begin{aligned}(4\pi)^2 \Pi_{RR}(q, i\omega) &= -\int_{-\infty}^{\infty} \frac{dq'}{2\pi} T \sum_{i\nu_n} \tilde{S}_R(q', i\nu_n) \\ &\quad \times \tilde{S}_R(q - q', i\omega - i\nu_n) \\ &\approx \int_{-\infty}^{\infty} \frac{dq'}{2\pi} \frac{q'(q - q')}{i\omega - v_s q - \Sigma_{q'} - \Sigma_{q-q'}} \\ &\quad \times [n_B(v_s q') - n_B(v_s q' - v_s q)], \end{aligned} \tag{74}$$

where $n_B(\omega) = 1/(e^{\omega/T} - 1)$ and $\Sigma_q = \Sigma_q(T) = \Sigma(q, v_s q, T)$. The decay rate for the spin boson at finite temperature is the well-known spin current relaxation rate[31]

$$\frac{1}{\tau_s(T)} = -\operatorname{Im} \Sigma_q^{\text{ret}} \approx \frac{\pi}{2}[g(T)]^2 T, \tag{75}$$

where $g(T) \approx g/[1 + g \ln(T_F/T)]$, with $T_F \sim m v_F^2$, is the coupling constant at scale T. The finite temperature result for the spin peak in this approximation is then

$$\delta A(q, \omega, T) \approx \frac{K_c}{48\pi} \frac{(\alpha_- + \alpha_+)^2 q^3 F(q,T) \tau_s}{1 + [(\omega - v_s q)\tau_s/2]^2}, \tag{76}$$

where

$$F(q,T) = 6 \int_{-\infty}^{\infty} du u(1-u)\{n_B(v_s q u) - n_B[v_s q(u-1)]\} \tag{77}$$

such that $F(q, T \to 0) = 1$. Since we neglected band curvature effects in the spin boson propagator, this approximation is only valid for $1/\tau_s(T) \gg \gamma q^3$. In Eq. (74), we also assumed $1/\tau_s(T) \ll v_s q$. Therefore we expect that the line shape of the spin peak at finite temperature be well described by a Lorentzian for a range of q that scales linearly with temperature, $q \sim T/v_s$, such that $T/g(T) \ll (v_s^3/\gamma)^{1/2}$.

More generally, for fixed q there is a crossover temperature T^* given by the condition $1/\tau_s(T^*) \sim \gamma q^3$ at which the line shape of the spin peak goes from highly asymmetric (with a peak near the zero-temperature threshold) below T^* to approximately Lorentzian in the diffusion-dominated regime above T^*.

V. APPLICATION TO THE DRAG RESISTIVITY

Finally, as an application of our results for the DCSF, in this section we will discuss the density and temperature dependence of the drag resistivity in Eq. (1). Here we restore the index $i=1,2$ for properties of the drive wire and drag wire, respectively. Note that Eq. (1) is symmetric under the exchange of drive and drag wires. We may then assume $v_{c1}\leq v_{c2}$. We envision an experiment in which the electron density of the drag wire is varied while the one in the drive wire is kept fixed. In principle, this could be achieved with vertically coupled wires whose densities are tuned independently by top and back gates. We can think that the sharply peaked DCSF of the drive wire is the reference for integrating Eq. (1) in the (q,ω) plane, and approximate

$$r \approx \frac{U^2}{4\pi^3 \nu_1 \nu_2 T}\int_0^\infty dq \frac{q^2}{\sinh^2(v_{c1}q/2T)} \times \int_0^\infty d\omega A_1(q,\omega)A_2(q,\omega). \tag{78}$$

Clearly, the forward scattering contribution to the drag resistivity is maximum for ideal density matching, $v_{c1}=v_{c2}$,[34] in which case it is dominated by the overlap of the charge peaks of the two wires over modes with $\omega \approx v_{ci}q \sim T \ll T_F$. The temperature dependence in this case is the same as for spinless fermions,[10] $r\sim T^2$ for $m|v_{c1}^2-v_{c2}^2| \ll T \ll T_F$. Also like the result for spinless fermions, a much weaker response, $r \sim T^5$, is obtained for general density mismatch in the regime $T \ll m|v_{c1}^2-v_{c2}^2|$, from the overlap of the charge peak for one wire with the tails of the DCSF for the other wire.

The new effect due to the spin degree of freedom is related to the presence of a spin peak in the DCSF illustrated in Fig. 3. It suggests that the drag resistivity can be enhanced when the electron densities in the wires are rather different but the charge peak of one wire overlaps with the spin peak of the other wire. This happens over an extended region in the (q,ω) plane if $v_{c1}=v_{s2}$. The interpretation is that under this condition holons in wire 1 can efficiently scatter off spinons in wire 2, which in their turn transfer momentum to holons in the same wire.

Let us discuss the temperature dependence of the drag resistivity when $v_{c1}=v_{s2}$. We are interested in the regime $T \ll mv_{c1}(v_{c2}-v_{c1})$, where spin-charge separation may be measurable. According to the result in Sec. IV E, the spin peak $\delta A(q,\omega,T)$ for values of q that scale linearly with T assume a Lorentzian line shape at low temperatures such that $T/g_2(T) \ll (v_{s2}^3/\gamma_2)^{1/2}$. The width of the charge peak for wire 1 for $q\sim T/v_{s2}$ is of order $\eta_{-,1}T^2/v_{s2}v_{c1}$. If the temperature is also low enough that $T/[g_2(T)]^2 \ll v_{c1}v_{s2}/\eta_{-,1} \sim T_F$, the spin peak for wire 2 is broader than the charge peak for wire 1. Using Eq. (72) for wire 1 and Eq. (76) for wire 2, we find that in this regime the drag resistivity in Eq. (78) scales like $r\sim T^5/[g_2(T)]^2$. However, if the value of $g_2(T)$ is small even at intermediate temperatures, there will be, in general, a temperature regime $g_2(v_{s2}^3/\gamma_2)^{1/2} \ll T \ll mv_{c1}(v_{c2}-v_{c1})$ where diffusion is not effective, in the sense that for $q\sim T/v_{s2}$ the broadening of the spin peak due to diffusion is smaller than the one due to band curvature. In this case, the spin peak for wire 2 is narrower than the charge peak for wire 1 for the same value of $q \ll k_{Fi}$. Therefore, the integral in Eq. (78) can be evaluated by considering that the entire spectral weight of the spin peak is inside the charge peak. In this regime, the drag resistivity in Eq. (78) scales like $r\sim T^4$. In summary

$$r \sim \begin{cases} T^5 \ln^2\dfrac{T_F}{T} & T \ll g_2(T)\sqrt{\dfrac{(v_{s2})^3}{\gamma_2}}, [g_2(T)]^2 T_F \\ T^4 & g_2\sqrt{\dfrac{(v_{s2})^3}{\gamma_2}} \ll T \ll mv_{c1}(v_{c2}-v_{c1}). \end{cases} \tag{79}$$

Notice that in the low-temperature limit diffusion suppresses the drag by making the spin peak broader than the charge peak. Nevertheless, even in the spin-diffusion regime the smallness of $g_2(T)\sim 1/\ln(T_F/T)$ makes the drag larger than the background contribution from the tails of the DCSF, which scales like $r\sim T^5$, as discussed above.

In order to compute the expression in Eq. (78), we have used the same strength of the electron-electron interaction $\tilde{V}_0$ and $\tilde{V}_{2k_F}$ for both wires. We estimated the parameters of the DCSF in each wire using the phenomenological relations in Sec. III, expanding to first order in the interaction. The finite temperature $A_i(q,\omega)$ are approximated by the sum of a dominant charge peak given by Eq. (72) and a smaller spin peak given by the Lorentzian in Eq. (76). For modes with $q \sim T/v_{c1}$ that contribute to the integral in Eq. (78) but are not in the regime $\gamma q^3 \ll 1/\tau_s(T)$, the Lorentzian is not a good approximation for the line shape of the spin peak (which must become asymmetric with a peak near the lower edge of the two spinon spectrum). However, the drag resistivity is not sensitive to the detailed line shape since in this regime the spin peak is much narrower than the charge peak for the same q and what matters most is whether the spin peak for the drag wire falls inside the charge peak for the drive wire.

Figure 5 illustrates the dependence of the drag resistivity on the density mismatch between the two wires, param-

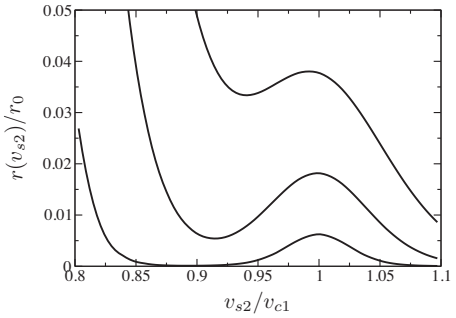

FIG. 5. Drag resistivity as a function of the spin velocity v_{s2} in the drag wire for three values of temperature: $T/(k_{F1}^2/m)=0.03,0.05,0.07$ (bottom to top). In this graph we set $\tilde{V}_0/(\pi v_{F1})=0.4$ and $\tilde{V}_{2k_F}/(\pi v_{F1})=0.1$ in the weak coupling expressions for v_{ci}, v_{si}, K_{ci}, η_{-i}, and $\kappa_{\pm i}$ for wires $i=1,2$, using equations in Sec. III. The value of $r(v_{s2})$ is normalized by the value at zero-density mismatch, $r_0=r(v_{s2}=v_{s1})$, for each temperature. Notice the peak in r when the spin velocity of the drag wire matches the charge velocity of the drive wire, $v_{s2}\approx v_{c1}$.

etrized by the ratio v_{s2}/v_{c1}. The effect of spinon-assisted Coulomb drag is observed as a small peak in the drag resistivity when the wire densities are such that $v_{s2} \approx v_{c1}$. The height of the peak relative to the dominant response at zero-density mismatch ($v_{s2} \approx v_{s1}$) increases with increasing temperature. This is because, as temperature increases, modes with larger q, for which the spin peak in the DCSF have relatively larger spectral weight, start to contribute to the integral in Eq. (78). On the other hand, increasing temperature also broadens the dominant peak observed at $v_{s2} \approx v_{s1}$, which eventually obscures the smaller peak at $v_{s2} \approx v_{c1}$. Therefore, it seems that the contribution of spinons to Coulomb drag would most likely be observed as a shoulder in the density dependence of the drag resistivity at intermediate temperatures.

VI. CONCLUSIONS

We have studied the dynamic charge response for spin-1/2 fermions in one dimension beyond the usual linear dispersion approximation of Luttinger liquid theory. Unlike the spinless case, the limits of small momentum q and weak electron-electron interactions $\tilde{V}_0$ do not commute. This is due to the interplay of spin-charge separation and band-curvature effects. The problem of calculating the dynamical charge-structure factor for electrons with mass m in the regime $q \ll m\tilde{V}_0$ cannot be approached by perturbation theory in the electron-electron interactions. We have used a bosonized Hamiltonian and discussed the effects of irrelevant perturbations associated with band curvature. We determined phenomenological relations for the coupling constants of these perturbations, including the ones that couple charge and spin dynamics. The renormalization group equations for the irrelevant operator denoted by κ_3, which couples charge and spin and mixes right- and left-moving spin modes, shows that its effective coupling constant has a nontrivial logarithmic scaling in the low-energy limit.

Based on a picture in which collective charge and spin modes can be refermionized into spinless fermions (holons and spinons, respectively) with nonlinear dispersion, we presented an approximate line shape for the dynamic charge-structure factor valid in the long wavelength limit. As a function of frequency, the dynamic charge-structure factor has a dominant charge peak associated with two-holon excitations, whose width scales like q^2. However, the spectral weight extends down to a lower threshold described as a two-spinon excitation. We calculated the exponent of the power-law singularity at this lower threshold and found that in the limit $q \to 0$ it converges to the universal value $\mu_{s-} = -1/2 + \mathcal{O}(q^2)$, which depends only on spin SU(2) symmetry. We expect that the spectral weight near this lower threshold is largest within a two-spinon continuum, giving rise to a spin peak in the charge-structure factor. There is also a tail of the spin peak above the two-spinon continuum. The coupling between spin and charge in the vicinity of the charge mass shell gives rise to a decay rate for the holon at order q^3. This decay rate is responsible for rounding-off singularities at intermediate thresholds such as the edges of the two-holon continuum, regardless of the integrability of the model.

At finite temperature, an important difference between charge and spin excitations is that the latter are damped by diffusion. In the dynamic charge-structure factor this effect is manifest in the Lorentzian broadening of the spin peak in the regime where the spin current decay rate is large compared to the band-curvature energy scale for the spinons.

These results allowed us to calculate the Coulomb drag response between two quantum wires, taking into account the spin degree of freedom. In comparison with the result for spinless fermions studied in Ref. 10, there is an additional effect (spinon-assisted Coulomb drag) due to spin-charge coupling: at low temperatures the drag resistivity as a function of density mismatch has a peak when the charge velocity of one wire matches the spin velocity of the other. The temperature dependence of this drag peak has signatures of spin diffusion.

Note added. After this work had been submitted, Ref. 35 appeared with related results for the exponent of edge singularities at arbitrary momenta.

ACKNOWLEDGMENTS

We acknowledge helpful discussions with J. M. P. Carmelo, L. I. Glazman, A. Imambekov, and T. L. Schmidt. This research was supported by the NSF under Grant No. PHY05-51164 (R.G.P.), by NSERC (E.S.), and the A. v. Humboldt Foundation (E.S.). We thank the authors of Ref. 35 for pointing out the relation in Eq. (71).

APPENDIX: CALCULATION OF THE LOWER-EDGE EXPONENT

We provide details for the calculation of the exponent of the power-law singularity in the DCSF at $\omega = \omega_{s-}(q)$ at zero temperature. While the asymptotic value $\mu_{s-}(q \to 0) = -1/2$ is universal and depends only on SU(2) symmetry, following the argument of Ref. 25, we also obtain the q^2 correction due to spin-charge coupling.

As mentioned in Sec. IV C, the lower edge of the spectrum is the same for the DCSF and for the DSSFs, defined as

$$S^{ab}(q,\omega) = \int_0^L dx e^{-iqx} \int_{-\infty}^{+\infty} dt e^{i\omega t} \langle S^a(x,t) S^b(0,0) \rangle. \quad \text{(A1)}$$

Here $\mathbf{S}(x) = \Psi^\dagger(x) \frac{\boldsymbol{\tau}}{2} \Psi(x)$, with $\boldsymbol{\tau}$ the vector of Pauli matrices, is the spin-density operator. Its long-wavelength components are represented by $\mathbf{S} = \mathbf{J}_L + \mathbf{J}_R$. For fixed q, the lower threshold below which the DSSFs (both longitudinal and transverse) vanish is controlled by a deep spinon excitation with energy $\omega_{s-}(q) = \epsilon_s(q)$.

The components of $\mathbf{S}$ satisfy SU(2) commutation relation

$$[S^a(x), S^b(x')] = i\varepsilon^{abc} S^c(x) \delta(x - x'). \quad \text{(A2)}$$

We will refermionize the spin density to spinless fermions. This can be done using an inverse Jordan-Wigner transformation in the continuum

$$S^z(x) = \Psi_s^\dagger(x) \Psi_s(x) + \text{const.}, \quad \text{(A3)}$$

$$S^+(x) = \Psi_s^\dagger(x) e^{i\pi \int_{-\infty}^{\infty} dx'\, \theta(x-x') S^z(x')}, \tag{A4}$$

where Ψ_s is a spinless fermionic spinon field, which obeys anticommutation relations $\{\Psi_s(x), \Psi_s^\dagger(x')\} = \delta(x-x')$, and $\theta(x)$ is the left-continuous Heaviside step function with $\theta(0)=0$.

A generic spin Hamiltonian that is a function of the local spin density and respects SU(2) symmetry takes the form

$$\mathcal{H}_s = C_1 \mathbf{S}\cdot\mathbf{S} + C_2 \partial_x \mathbf{S}\cdot\partial_x \mathbf{S} + \cdots, \tag{A5}$$

where $\cdots$ stands for higher order irrelevant operators. By means of Eqs. (A3) and (A4), this maps onto a model of interacting spinons. The precise form of the spinon Hamiltonian is not essential here but it must be such that in the low energy limit it yields the same equal-time correlation functions as the spin part of the Luttinger model in Eq. (7). This is directly accomplished if the model in Eq. (7) is recovered by bosonization of Ψ_s, analogously to the bosonization of the XXZ model.[23] In this approach, the SU(2) symmetric model corresponds to strong interactions between spinons. Here we assume that the effective model for the spinons in the metallic case can be approached in the same way as the effective model for the Heisenberg spin chain, namely, by starting from a generalized model of weakly interacting spinless fermions where we can expand the dispersion about the Fermi points to bosonize the low-energy degrees of freedom. SU(2) symmetry is only imposed at the end, on the results for the spin-spin correlation functions, to fix the parameters of the effective model. [It is conceivable that the strength of the spinon-spinon interaction could be tuned in a microscopic model for a metal with spin U(1) symmetry and that such weakly interacting limit could be realized.] In addition to the interactions in the effective spinon model, we must account for the coupling to gapless charge modes. For the purpose of deriving the exponent at the spinon edge, the latter can be described by bosonic fields $\varphi^c_{R/L}$ at all steps and need not be refermionized. The spin-charge coupling is then equivalent to spin-phonon coupling in spin chains.

Let us consider that in the ground state the spinons form a Fermi sea with a particle-hole symmetric band (due to spin inversion symmetry $S^z \to -S^z$). The elementary $S^z=0$ excitations are particle-hole pairs in the spinon Fermi sea. Similarly, there are particle-hole excitations in the holon Fermi sea but in our low-energy effective model for the lower edge these are treated as charge bosons (since we can neglect band curvature for the holons). This picture is supported by the Bethe ansatz solution of the Yang-Gaudin or Hubbard models. We assume that we can start from a model of noninteracting spinons with dispersion $\epsilon^{(0)}_{s,R/L}(k) \approx \pm(v_s^{(0)}k - \gamma^{(0)}k^3 + \cdots)$ about the Fermi points $\pm k_F$. That the spinon Fermi wave vector is given by $k_{Fs}=k_F$ follows from the periodicity of the spin-excitation spectrum, which is gapless at momentum $2k_F$.[28] Another interpretation is that in this approach the number of spinons

$$\int_0^L dx \Psi_s^\dagger(x)\Psi_s(x) = k_{Fs}L/\pi = N/2, \tag{A6}$$

is fixed by the condition that the state constructed by adding (removing) $N/2$ spinons to the ground state is a fully polarized state with N spins up (N spins down), which no more spinons can be added to (removed from).

Expanding the spinon field about $\pm k_F$, $\Psi_s \sim e^{ik_F x}\psi_{sR} + e^{-ik_F x}\psi_{sL}$, we can write a phenomenological Hamiltonian density of the form

$$\mathcal{H} = \mathcal{H}_s + \mathcal{H}_c + \mathcal{H}_{cs}, \tag{A7}$$

where

$$\mathcal{H}_s = \psi^\dagger_{sR}(-iv_s^{(0)}\partial_x + i\gamma^{(0)}\partial_x^3)\psi_{sR} + \psi^\dagger_{sL}(iv_s^{(0)}\partial_x - i\gamma^{(0)}\partial_x^3)\psi_{sL} + \mathcal{H}_s^{int} \tag{A8}$$

is the spinon Hamiltonian with spinon-spinon interactions contained in $\mathcal{H}_s^{int}$, $\mathcal{H}_c$ is the charge Hamiltonian given by the charge part of Eq. (7), and $\mathcal{H}_{cs}$ contains spinon-holon interactions. Due to spinon particle-hole symmetry, the latter can only contain irrelevant operators (dimension three and higher), for instance, $\psi^\dagger_{s,R/L}\partial_x\psi_{s,R/L}\partial_x\varphi^c_{R/L}$.

The parameters $v_s^{(0)}$ and $\gamma^{(0)}$ are renormalized by interactions (both spinon-spinon and spinon-holon). We denote the parameters of the exact spinon dispersion by v_s and γ. As usually done for v_s, the exact γ can be extracted from the Bethe ansatz solution in the case of integrable models. For repulsive electron-electron interactions, we expect $v_s < v_c$, where v_c is the exact charge velocity. In this case, the lower edge of the spectrum of *any* dynamical correlation function at small momentum q (such that $|\gamma q^2| \ll v_s < v_c$) is controlled by the spinon branch line, with a single "deep spinon" with energy $\epsilon_s(q) \equiv \epsilon_{sR}(q) \approx v_s q - \gamma q^3$ and a certain number of spinon or holon excitations at the Fermi points.

Whether or not the band curvature of the spinon dispersion can be neglected in the calculation of dynamical quantities depends on the frequency range of interest.[7] Far enough from the threshold, for $|\omega - \epsilon_s(q)| \gg \gamma q^3$, we are allowed to drop the band curvature operators and the dynamics is captured by Luttinger liquid theory. We can bosonize $\psi_{s,R/L}$ in the standard way,[23] using $\psi_{s,R/L} \sim e^{-i\sqrt{2\pi}\phi^s_{R/L}}/\sqrt{2\pi\alpha}$, with chiral bosonic fields $\phi^s_{R/L}$ and α a short distance cutoff. The quadratic Hamiltonian in terms of spin bosons is diagonalized by a transformation to

$$\varphi^s_L \pm \varphi^s_R = K^{\pm(1/2)}(\phi^s_L \pm \phi^s_R), \tag{A9}$$

where K is the Luttinger parameter for the spinons. The latter is fixed by SU(2) symmetry. In Abelian bosonization, we write $S^z \sim \partial_x\varphi^s_R - \partial_x\varphi^s_L$, which has scaling dimension 1. For S^+, we bosonize the fermion and string operators in Eq. (A4) and obtain

$$S^+ \sim e^{-i\sqrt{2\pi}(\sqrt{K}-(1/2\sqrt{K}))\varphi^s_R} e^{i\sqrt{2\pi}(\sqrt{K}+(1/2\sqrt{K}))\varphi^s_L}, \tag{A10}$$

which has scaling dimension $K+1/4K$. Demanding that this dimension is equal to 1 gives $K=1/2$.

On the other hand, for $|\omega - \epsilon_s(q)| \ll \gamma q^3$, the behavior of dynamical correlation functions is sensitive to the band curvature energy scale. In this regime, it is important to consider that spinons created near the threshold with energy $\epsilon_s(q)$ travel with a different velocity than spinons at the spinon Fermi surface. It has become standard to treat this type of problem using quantum impurity models in analogy with the

x-ray edge singularity.[16] In order to describe the deep spinon threshold, we expand the spinon field with low and high energy subbands

$$\psi_{sR} \sim \psi_{sr} + e^{-iqx} d_{s1}^{\dagger} + e^{iqx} d_{s2}. \tag{A11}$$

(In the main text we considered only one type of d-particle for simplicity.) The subband momentum cutoff is taken to be small compared to q. For $q>0$, we consider deep holes with momentum about k_F-q and high-energy particles with momentum about k_F+q. These two types of excitations are degenerate as a consequence of particle-hole symmetry. The low energy ψ_{sr} and ψ_{sl} fields are then bosonized while $d_{s1,2}$ are treated as mobile impurities. We denote by $\varphi_{r/l}^{s}$ the chiral spin boson fields with the reduced cutoff at scale q. The interactions among low and high energy spinons and low-energy charge bosons can be described by the effective Hamiltonian density

$$\mathcal{H} = \mathcal{H}_c + \mathcal{H}_{s,\ell} + \mathcal{H}_d + \mathcal{H}_{sd} + \mathcal{H}_{cd}. \tag{A12}$$

Here $\mathcal{H}_c$ is the free charge boson Hamiltonian with reduced cutoff at scale q (fields denoted by $\varphi_{r/l}^{c}$). In the spin-only part of $\mathcal{H}$

$$\mathcal{H}_{s,\ell} = \frac{v_s}{2}[(\partial_x \varphi_r^s)^2 + (\partial_x \varphi_l^s)^2] \tag{A13}$$

is the Luttinger model for low energy spin excitations (here written in Abelian bosonization form),

$$\mathcal{H}_d = d_{s1}^{\dagger}[\epsilon_s(q) - iu\partial_x] d_{s1} + (1 \to 2) \tag{A14}$$

is the kinetic energy of the high-energy spinons with $u = u(q)$ the corresponding exact velocity and

$$\mathcal{H}_{sd} = \frac{1}{\sqrt{4\pi}}(V_l \partial_x \varphi_l^s - V_r \partial_x \varphi_r^s)(d_{s2}^{\dagger} d_{s2} - d_{s1}^{\dagger} d_{s1}) \tag{A15}$$

is the coupling between high-energy spinons and low-energy spin bosons. The amplitudes V_r and V_l will be determined below.[10,24] Note that $\mathcal{H}_{sd}$ is invariant under the particle-hole transformation $\psi_{s,R/L} \to \psi_{s,R/L}^{\dagger}$, which takes $\varphi_{r/l}^{s} \to -\varphi_{r/l}^{s}$, $d_{s1} \leftrightarrow d_{s2}$. Here we have neglected the backscattering operator g in Eq. (7), which becomes marginal at the SU(2) point; however, we point out that it might be important for logarithmic corrections to edge singularities, which are known to exist for the DSSF of the Heisenberg spin chain.[26] The spin-charge coupling in $\mathcal{H}$ is given by

$$\mathcal{H}_{cd} = \frac{1}{\sqrt{2\pi K_c}}(V_l^c \partial_x \varphi_l^c - V_r^c \partial_x \varphi_r^c)(d_{s1}^{\dagger} d_{s1} + d_{s2}^{\dagger} d_{s2}). \tag{A16}$$

The amplitudes $V_{r/l}^{c}$ in Eq. (A16) stem from operators such as $\psi_{sR}^{\dagger} \partial_x \psi_{sR} \partial_x \varphi_{r/l}^{c}$, taking the high-energy mode in the expansion of ψ_R. As a result, $V_{r/l}^{c}$ scale like $\sim q$. The relation to the parameters in Eq. (50) is $V_{l/r}^{c} = \pm\sqrt{2K_c \pi q \kappa_{\pm}'}$.

Hamiltonian $\mathcal{H}$ can be diagonalized by a unitary transformation of the form $\tilde{H} = UHU^{\dagger}$ where $U = U_1 U_2$ with

$$U_{1,2} = e^{-i\int dx(\mp \gamma_r \varphi_r^s + \gamma_l \varphi_l^s/\sqrt{\pi} + \gamma_r^c \varphi_r^c + \gamma_l^c \varphi_l^c/\sqrt{2\pi K_c}) d_{s1,2}^{\dagger} d_{s1,2}} \tag{A17}$$

with

$$\gamma_{l/r} = -\frac{V_{l/r}}{2(v_s \pm u)}, \quad \gamma_{l/r}^{c} = -\frac{V_{l/r}^{c}}{v_c \pm u} \approx -\frac{V_{l/r}^{c}}{v_c \pm v_s}. \tag{A18}$$

This transformation takes

$$d_{s1,2} \to \tilde{d}_{s1,2} e^{-i(\mp \gamma_r \varphi_r^s + \gamma_l \varphi_l^s/\sqrt{\pi} + \gamma_r^c \varphi_r^c + \gamma_l^c \varphi_l^c/\sqrt{2\pi K_c})}, \tag{A19}$$

where $\tilde{d}_{s1,2}$ are free (up to irrelevant operators). The γ's are interpreted as phase shifts at the spinon and holon Fermi points due to the creation of a high-energy spinon.

The exponents for the edge singularities are then calculated using the methods of Refs. 16 and 24. The threshold for the longitudinal DSSF $S^{zz}(q,\omega)$ is given by the correlation function for the operator that creates a particle-hole pair of spinons with a hole at k_F and a particle at k_F+q (or equivalently a hole at k_F-q and a particle at k_F)

$$B_z^{\dagger} = d_{s2}^{\dagger} \psi_{sr} \sim \tilde{d}_{s2}^{\dagger} e^{-i\sqrt{2\pi}(\lambda_r \varphi_r^s + \lambda_l \varphi_l^s + \lambda_r^c \varphi_r^c + \lambda_l^c \varphi_l^c)} \tag{A20}$$

with

$$\lambda_r = \frac{1}{\sqrt{2}}\left(\frac{3}{2} - \frac{\gamma_r}{\pi}\right),$$

$$\lambda_l = \frac{1}{\sqrt{2}}\left(\frac{1}{2} - \frac{\gamma_l}{\pi}\right) \tag{A21}$$

and

$$\lambda_{r/l}^{c} = -\frac{1}{2\sqrt{K_c}} \frac{\gamma_{r/l}^{c}}{\pi}. \tag{A22}$$

Using Eq. (A20), we calculate the Fourier transform of the correlation function $\langle B_z(x,t) B_z^{\dagger}(0,0)\rangle$ and find a power-law singularity $S^{zz}(q,\omega) \sim (\omega - \omega_{s-})^{\mu_{zz}}$ with exponent

$$\begin{aligned}\mu_{zz} &= -1 + (\lambda_r)^2 + (\lambda_l)^2 + (\lambda_r^c)^2 + (\lambda_l^c)^2 \\ &= -1 + \frac{1}{2}\left(\frac{3}{2} - \frac{\gamma_r}{\pi}\right)^2 + \frac{1}{2}\left(\frac{1}{2} - \frac{\gamma_l}{\pi}\right)^2 \\ &\quad + \frac{1}{4K_c}\left[\left(\frac{\gamma_r^c}{\pi}\right)^2 + \left(\frac{\gamma_l^c}{\pi}\right)^2\right].\end{aligned} \tag{A23}$$

The last term amounts to an orthogonality catastrophe contribution to the exponent due to coupling of the $d_{s1,2}$ particles to gapless charge modes.

Now consider the transverse DSSF $S^{+-}(q,\omega)$. In this case the operator Eq. (A4) creates a particle and a string

$$B_{+}^{\dagger}(x) \sim d_{s2}^{\dagger} e^{-i\sqrt{\pi/2}(\phi_l^s - \phi_r^s)} \sim \tilde{d}_{s2}^{\dagger} e^{-i\sqrt{2\pi}(\lambda_r' \varphi_r^s + \lambda_l' \varphi_l^s + \lambda_r^c \varphi_r^c + \lambda_l^c \varphi_l^c)} \tag{A24}$$

with

$$\lambda_r' = \frac{1}{\sqrt{2}}\left(\frac{1}{2} - \frac{\gamma_r}{\pi}\right), \quad \lambda_l' = \frac{1}{\sqrt{2}}\left(-\frac{1}{2} - \frac{\gamma_l}{\pi}\right). \tag{A25}$$

The Fourier transform of the correlation function $\langle B_+(x,t)B_+^\dagger(0,0)\rangle$ leads to $S^{+-}(q,\omega)\sim(\omega-\omega_{s-})^{\mu_{+-}}$ with the exponent

$$\mu_{+-} = -1 + \frac{1}{2}\left(\frac{1}{2} - \frac{\gamma_r}{\pi}\right)^2 + \frac{1}{2}\left(\frac{1}{2} + \frac{\gamma_l}{\pi}\right)^2 + \frac{1}{4K_c}\left[\left(\frac{\gamma_r^c}{\pi}\right)^2 + \left(\frac{\gamma_l^c}{\pi}\right)^2\right]. \tag{A26}$$

SU(2) symmetry implies that $\mu_{zz}=\mu_{+-}$ but this is only one equation. However, we can actually get infinitely many equations by imposing SU(2) symmetry for the singularities that differ from the above by zero-energy excitations in which spinons are transferred between the Fermi points. These are created by electron backscattering processes in the language of spin-1/2 fermions, which are Umklapp processes for spinons

$$(\psi_{sr}^\dagger \partial_x \psi_{sr}^\dagger \psi_{sl}\partial_x\psi_{sl})^n \sim e^{-i\sqrt{4\pi}n(\varphi_l^s-\varphi_r^s)}, \tag{A27}$$

where n is an integer [$n<0$ on the right-hand side of Eq. (A27) corresponds to the Hermitian conjugate of the left-hand side]. The excitations that differ in momentum by $2nk_F$ have thresholds at the same frequency $\omega_{s-}(q)$ because the spin spectrum is periodic in momentum with period $2k_F$. The exponents for $|q-2nk_F|\ll k_F$ are given by

$$\mu_{zz,n} = -1 + (\lambda_{r,n})^2 + (\lambda_{l,n})^2 + (\lambda_r^c)^2 + (\lambda_l^c)^2,$$

$$\mu_{+-,n} = -1 + (\lambda_{r,n}')^2 + (\lambda_{l,n}')^2 + (\lambda_r^c)^2 + (\lambda_l^c)^2,$$

where

$$\lambda_{r,n} = \frac{1}{\sqrt{2}}\left(-2n + \frac{3}{2} - \frac{\gamma_r}{\pi}\right),$$

$$\lambda_{l,n} = \frac{1}{\sqrt{2}}\left(+2n + \frac{1}{2} - \frac{\gamma_l}{\pi}\right),$$

$$\lambda_{r,n}' = \frac{1}{\sqrt{2}}\left(-2n + \frac{1}{2} - \frac{\gamma_r}{\pi}\right),$$

$$\lambda_{l,n}' = \frac{1}{\sqrt{2}}\left(+2n - \frac{1}{2} - \frac{\gamma_l}{\pi}\right). \tag{A28}$$

The condition $\mu_{zz,n}=\mu_{+-,n}$ is satisfied for all n if and only if $\gamma_r/\pi=\gamma_l/\pi=1/2$. With this result, the exponent in the lower edge of the DSSFs (or the DCSF) for $q\ll k_F$ becomes

$$\mu_{s-} = \mu_{zz} = \mu_{+-} = -\frac{1}{2} + \frac{1}{4K_c}\left[\left(\frac{\gamma_r^c}{\pi}\right)^2 + \left(\frac{\gamma_l^c}{\pi}\right)^2\right]. \tag{A29}$$

With $\gamma_{l/r}^c$ given in Eq. (A18) and $V_{l/r}^c = \pm\sqrt{2K_c}\pi q\kappa_\pm'$ fixed as explained in Sec. IV C, we obtain the final result in Eq. (56).

[1] A. M. Tsvelik, *Quantum Field Theory in Condensed Matter Physics* (Cambridge University Press, Cambridge, 1995).
[2] O. M. Auslaender, A. Yacoby, R. de Picciotto, K. W. Baldwin, L. N. Pfeiffer, and K. W. West, Science **295**, 825 (2002).
[3] Y. Jompol, C. J. B. Ford, J. P. Griffiths, I. Farrer, G. A. C. Jones, D. Anderson, D. A. Ritchie, T. W. Silk, and A. J. Schofield, Science **325**, 597 (2009).
[4] B. J. Kim, H. Koh, E. Rotenberg, S.-J. Oh, H. Eisaki, N. Motoyama, S. Uchida, T. Tohyama, S. Maekawa, Z.-X. Shen, and C. Kim, Nat. Phys. **2**, 397 (2006).
[5] C. Nayak, K. Shtengel, D. Orgad, M. P. A. Fisher, and S. M. Girvin, Phys. Rev. B **64**, 235113 (2001).
[6] M. Sassetti and B. Kramer, Phys. Rev. Lett. **80**, 1485 (1998); D. W. Wang, A. J. Millis, and S. Das Sarma, *ibid.* **85**, 4570 (2000).
[7] A. Imambekov and L. I. Glazman, Science **323**, 228 (2009).
[8] Yu. V. Nazarov and D. V. Averin, Phys. Rev. Lett. **81**, 653 (1998).
[9] P. Debray, V. Zverev, O. Raichev, R. Klesse, P. Vasilopoulos, and R. S. Newrock, J. Phys.: Condens. Matter **13**, 3389 (2001); M. Yamamoto, M. Stopa, Y. Tokura, Y. Hirayama, and S. Tarucha, Science **313**, 204 (2006).
[10] M. Pustilnik, E. G. Mishchenko, L. I. Glazman, and A. V. Andreev, Phys. Rev. Lett. **91**, 126805 (2003).
[11] A. V. Rozhkov, Eur. Phys. J. B **47**, 193 (2005).
[12] R. G. Pereira, J. Sirker, J.-S. Caux, R. Hagemans, J. M. Maillet, S. R. White, and I. Affleck, Phys. Rev. Lett. **96**, 257202 (2006); J. Stat. Mech.: Theory Exp. (2007) P08022.
[13] D. Laroche, E. S. Bielejec, J. L. Reno, G. Gervais, and M. P. Lilly, Physica E **40**, 1569 (2008).
[14] T. Stöferle, H. Moritz, C. Schori, M. Köhl, and T. Esslinger, Phys. Rev. Lett. **92**, 130403 (2004).
[15] J. Peguiron, C. Bruder, and B. Trauzettel, Phys. Rev. Lett. **99**, 086404 (2007).
[16] M. Pustilnik, M. Khodas, A. Kamenev, and L. I. Glazman, Phys. Rev. Lett. **96**, 196405 (2006).
[17] D. N. Aristov, Phys. Rev. B **76**, 085327 (2007).
[18] S. Teber, Phys. Rev. B **76**, 045309 (2007).
[19] J. Cardy, *Scaling and Renormalization in Statistical Physics* (Cambridge University Press, Cambridge, 1996).
[20] The $\sqrt{2}$ factor was missed in Ref. 18.
[21] M. Gaudin, Phys. Lett. **24A**, 55 (1967); C. N. Yang, Phys. Rev. Lett. **19**, 1312 (1967).
[22] S. Lukyanov, Nucl. Phys. B **522**, 533 (1998).
[23] T. Giamarchi, *Quantum Physics in One Dimension* (Oxford University Press, New York, 2004).
[24] R. G. Pereira, S. R. White, and I. Affleck, Phys. Rev. Lett. **100**, 027206 (2008).
[25] A. Imambekov and L. I. Glazman, Phys. Rev. Lett. **102**, 126405 (2009).
[26] M. Karbach, G. Müller, A. H. Bougourzi, A. Fledderjohann, and K.-H. Mütter, Phys. Rev. B **55**, 12510 (1997).
[27] M. B. Zvonarev, V. V. Cheianov, and T. Giamarchi, Phys. Rev.

Lett. **99**, 240404 (2007).
[28] A. Kamenev and L. I. Glazman, Phys. Rev. A **80**, 011603(R) (2009).
[29] R. G. Pereira, S. R. White, and I. Affleck, Phys. Rev. B **79**, 165113 (2009).
[30] J. Voit, Phys. Rev. B **47**, 6740 (1993).
[31] L. Balents and R. Egger, Phys. Rev. B **64**, 035310 (2001).
[32] M. Polini and G. Vignale, Phys. Rev. Lett. **98**, 266403 (2007).
[33] M. Oshikawa and I. Affleck, Phys. Rev. B **65**, 134410 (2002).
[34] For $\nu_1 = \nu_2$ and low-enough temperatures, the drag would be dominated by backscattering ($q \sim 2k_F$) processes; see Refs. 8 and 10.
[35] T. L. Schmidt, A. Imambekov, and L. I. Glazman, Phys. Rev. Lett. **104**, 116403 (2010).